Limberg, W.; Ebel, T.; Pyczak, F.; Oehring, M.; Schimansky, F.P.:

Influence of the sintering atmosphere on the tensile properties of MIM-processed Ti 45Al 5Nb 0.2B 0.2C

In: Materials Science and Engineering A (2012) Elsevier

DOI: 10.1016/j.msea.2012.05.047

Influence of the sintering atmosphere on the tensile properties of MIM-processed Ti 45Al 5Nb 0.2B 0.2C

W. Limberg*, T. Ebel, F. Pyczak, M. Oehring, F. P. Schimansky
Institute of Materials Research, Helmholtz-Zentrum Geesthacht, Centre for Materials and Coastal Research, Max-Planck-Strasse 1, D-21502 Geesthacht, Germany

**Corresponding author. Tel. +49-4152-871915, Fax +49-4152-871920, E-mail: wolfgang.limberg@hzg.de*

Abstract

In this study tensile test specimens were produced by metal injection moulding (MIM) of gas-atomized TNB-V5 alloy powder with the nominal composition Ti 45Al 5Nb 0.2B 0.2C (at. %). The specimens were sintered at 1500 °C under different atmospheres. The influence of the sintering atmosphere and the sintering time on the tensile properties, the microstructure and Al-sublimation were investigated. The residual porosity of the specimens increased proportionally with the applied argon gas pressure during sintering from 0.1 % for vacuum to 1.1 % for 80 kPa. Nevertheless, no relationship between the sintering pressure and the mechanical properties was found and ultimate tensile strengths (UTS) between 625 and 630 MPa with plastic elongations of 0.15 to 0.19 % at room temperature were determined.

Keywords: Titanium aluminides; Metal injection moulding; Aluminium evaporation; Porosity; Tensile properties

1. Introduction

In times of exploding energy costs caused by the shortage of fossil fuels, the development of combustion engines and gas turbines with higher efficiency has become increasingly important. It is therefore necessary to reduce the masses of rotating and oscillating parts in such engines. Titanium aluminides (TiAl) are attractive materials for this purpose due to their high specific strength, high stiffness and their high temperature strength up to 800 °C. Currently, TiAl-alloys are being introduced as low pressure turbine foils in an aero engine for passenger aircraft [1] despite certain materials drawbacks such as low room temperature ductility, fatigue strength and damage tolerance, to name but a few. Unfortunately, due to their low ductility, titanium aluminides are also difficult to process by conventional methods such as machining or forging, while casting leads to inhomogeneous microstructures [2]. In this respect, powder metallurgy (PM) is an attractive alternative production route, because fine microstructures without macro-segregation and having good chemical homogeneity can be obtained. Metal injection moulding (MIM) has the potential to be a cost-efficient, near net shape powder technique, especially, for complex shaped mass produced parts such as turbo charger wheels. However, MIM-processing of TiAl alloys is a novel production route and significant development is necessary to make it suitable for industrial applications, in particular in view of the low ductility and limited damage tolerance of the material. This paper will address some of the issues which should be considered here.

MIM-processing of fine TiAl powders is very demanding because of the high reactivity of TiAl with oxygen and nitrogen, which is accompanied by embrittlement of the material. The low diffusivity of TiAl requires high sintering temperatures close to the solidus to achieve a low residual porosity [3]. In addition the reactivity of TiAl with oxygen and nitrogen is extremely high at elevated temperature. Thus, attention must be paid to ensure absolutely clean processing conditions. These issues make sintering the most difficult step during MIM-processing of TiAl.

Another challenge is the avoidance of an inhomogeneous microstructure, especially in regions near the surface, because at the high sintering temperature up to 1500 °C, the sublimation of aluminium increases, which causes an acicular surface structure. Since sublimation of Al may be reduced by sintering at higher pressure, which in turn affects the sintering behaviour and the properties of the material the influence of the sintering atmosphere on microstructure, chemical homogeneity and tensile properties of MIM-processed Ti 45Al 5Nb 0.2B 0.2C was investigated in this study.

2. Experimental

2.1. Powder production

The alloy used for the experiments was TNB-V5 (Ti 45Al 5Nb 0.2B 0.2C, all in atomic percent). The alloy powder was produced by argon gas atomisation using the EIGA-technique (Electrode Induction Melting Gas Atomisation). Details on this technique have been published elsewhere [4]. The powder particles are spherically shaped and a certain number of satellites are observed (Figure 1). In spite of this amount of satellites the powder shows good free flowing properties. For Metal Injection Moulding the fine powder fraction with a particle size < 45 µm was separated by sieving. To prevent the powder from oxidation, the entire powder handling, from gas

atomisation to feedstock preparation, was performed under an argon atmosphere.

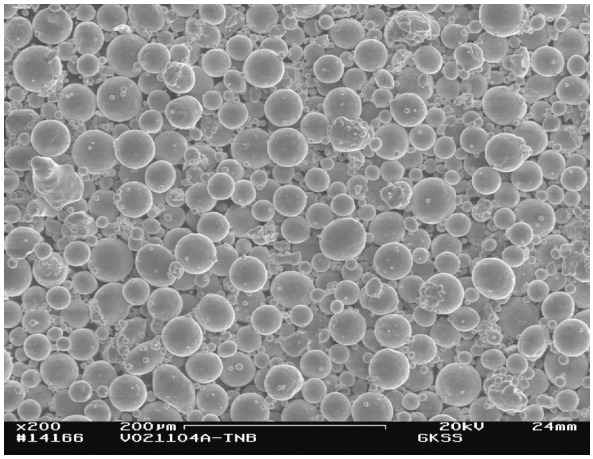

Fig. 1. *SEM-image of the gas atomised Ti 45Al 5Nb 0.2B 0.2C-powder (sieved fraction < 45 m).*

2.2. MIM-Processing

Feedstock preparation:

The binder used has the same composition as that already applied successfully for MIM of conventional titanium alloys. In the case of conventional titanium alloys use of this binder led to good mechanical properties of the sintered specimens [5]. The composition is 35 wt. % ethylene vinyl acetate (EVA), 60 wt. % paraffin wax (PW) and 5 wt. % stearic acid (SA). The feedstock, which contains 10 wt. % of this binder, was prepared by mixing powder and binder in a double Z-blade mixer (Femix KM 0,5 K) for two debinding machine, using heptane at 40 °C for 15 hours. Thermal debinding and sintering were performed in subsequent steps, using a cold-wall furnace with tungsten heating elements and molybdenum shield packs. The thermal debinding took place under a slight argon flow of 150 l/h at 500 Pa in the temperature range between 250 and 400 °C.

In our previous studies [3] a temperature of 1500 °C was found to be the optimum temperature for sintering the alloy TNB-V5. Sintering at lower temperatures e.g. at 1480 °C leads to insufficient densification and a coarse microstructure. At such lower temperatures the alloy TNB-V5 is not in the single β-phase region. This could be a possible reason for the coarse microstructure because grain refinement, which occurs during the $\beta \rightarrow \alpha$ solid state transformation is not possible. This is discussed in more detail with respect to the influence of the cooling rate on the colony size later. An increase of the sintering temperature to 1510 °C results in the formation of liquid phase. The specimens were therefore sintered at a temperature of 1500 °C for two different durations (1 and 2 h) under vacuum (10^{-3} Pa) or at 1500 °C for 2 h in argon atmospheres with three different pressures (10, 30 and 80 kPa). All specimens for tensile tests were cooled at a rate of 100 K/min from the sintering temperature down to 1000 °C.

hours at a temperature of 120 °C. In order to provide the argon atmosphere mentioned above the kneader was positioned inside a glove box.

Injection moulding:

Standard MIM tensile test specimens according to ISO 2740 (Figure 2) were injection moulded using a two-cavity mould on a conventional ARBURG 320 S 500-60 machine. An injection pressure of 80 MPa, an injection rate of 35 cm^3/s, an injection temperature of 112 °C and a mould temperature of 43 °C were found to be adequate for the injection process.

Fig. 2. *MIM tensile test specimens referring to ISO 2740 (sintered and green part), total length of the green part was 90 mm.*

Debinding and sintering:

The binder system employed here requires a two-stage debinding process: chemical debinding to extract the paraffin component and thermal debinding to crack and vaporise the remaining polyethylene. Chemical debinding was performed in a solvent

2.3. Tensile Tests

Tensile tests were performed in air at room temperature on a Schenck Trebel RM 100 tensile testing machine with a traverse speed of 0.2 mm/min. The gauge length was 30 mm and the gauge diameter 4.3 mm. The strain was measured by a laser extensometer (Fiedler Laser Scanner). Before tensile testing, the specimens were shot peened with ZrO_2 at a pressure of 800 kPa to suppress the influence of possibly existing incipient cracks by induced compressive stresses at the surface. However, comparative tensile tests carried out on MIM-specimens with and without additional shot peening, showed no significant differences in the tensile properties.

2.4. Characterisation

For light optical microscopy, the samples were mechanically ground and polished. These samples were also used for the porosity and colony size analysis. Here an Olympus microscope and Adobe Photoshop imaging software for plane section analysis were used. The colony sizes were measured by linear intercepts of colony boundaries according to ASTM E 112-96. Samples for scanning electron microscopy (SEM) were prepared by grinding and electropolishing. It is noted here that pores may appear larger in size in electropolished samples and

some of the borides can fall out of the specimen during electropolishing. Microstructural characterization by SEM was carried out using back-scattered electron (BSE) imaging in a Zeiss DSM962 and a LEO Gemini 1530 microscope. The concentration of metallic elements in selected specimen regions was analyzed using an energy dispersive X-ray spectroscopy (EDS) analysis system (Oxford INCA) attached to the Zeiss microscope. The EDS analyzer was calibrated using a ternary Ti-45Al-10Nb alloy standard. It should be noted that the measured concentrations of metallic elements appear to be a factor of 1.004 higher than present in the alloy due to the fact that the alloying elements B and C have not been included in the EDS analyses. Oxygen and nitrogen analyses were performed with a LECO melt extraction system.

3. Results and Discussions

3.1. Impurity Levels

The concentrations of oxygen and nitrogen were analysed on the alloy powder and on the MIM-manufactured specimens after sintering. They are listed in Table 1.

Sintering conditions	Oxygen [µg/g]	Nitrogen [µg/g]
2 h in Ar 80 kPa	1333	202
2 h in Ar 30 kPa	1353	170
2 h in Ar 10 kPa	1437	136
2 h in vacuum	1140	217
1 h in vacuum	1354	163
Alloy-powder	515	60

Table 1 *Impurity levels of MIM-TNB-V5 sintered at 1500 °C in different atmospheres compared to the used alloy powder.*

The oxygen content of the fine powder fraction <45 µm is very difficult to measure, because exposure to air for a short time cannot be avoided. Due to the large specific surface area, the fine powder is more susceptible to oxygen pick-up. This short time is sufficient to cause a massive increase in the oxygen concentration. The most reliable way to determine the impurity levels of the fine powder is therefore to analyze the specimens compacted by hot isostatic pressing (HIP) of the fine TNB-V5 alloy powder, which have been handled under argon or under vacuum prior to compaction by HIP. A further study [4] has shown, that the impurity levels of the fine powder measured on hot isostatically pressed specimens provides the same values as were determined for the coarse (> 355 µm) powder fraction. This verifies that impurity pick-up during the inert gas atomisation is the same for coarse as for fine powder. For this reason, the O_2 and N_2 analysis results given in Table 1 for the alloy powder were determined on the coarse powder fraction > 355 µm.

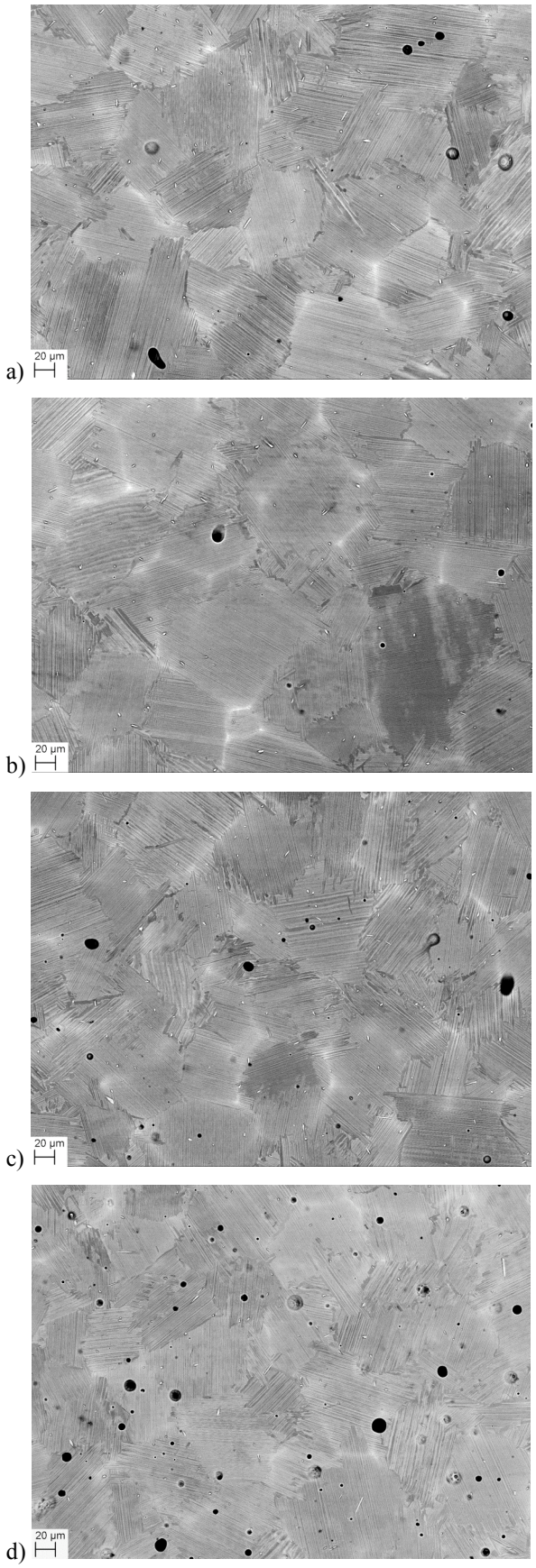

Fig. 3. *SEM-images of cross-sections of MIM-TNB-V5 specimens sintered at 1500 °C. (a) 1 h; vacuum, (b) 2 h; vacuum. (c) 2 h; 10 kPa Ar. (d) 2 h; 80 kPa Ar.*

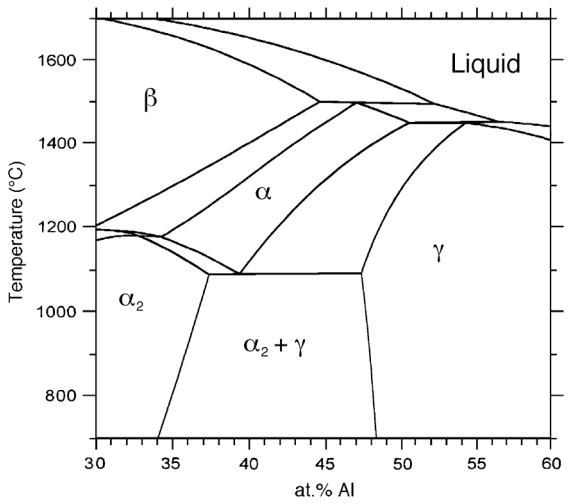

Fig. 4. *Detail of the calculated (ThermoCalc using commercial database TTTIAL) quasi-binary Ti–Al phase diagram including 5 at.% Nb.*

The MIM specimens show an average increase of the oxygen level of about 800 µg/g compared to the alloy powder. No obvious relationship between the oxygen content and the different sintering conditions is observed. The differences in oxygen level between the different MIM specimens seem to be caused by other differences in processing conditions e.g. contamination of the furnace from prior sintering runs.

With increasing argon pressure the nitrogen content increased from 136 µg/g at 10 kPa argon pressure to 202 µg/g at 80 kPa argon pressure. Thus, it seems that a relationship between the applied argon pressure during sintering and the nitrogen content exists. Surprisingly, the specimens which were sintered in vacuum showed a relatively high nitrogen content of 163 µg/g after 1 hour and of 217 µg/g after 2 hours. So it remains unclear whether nitrogen contamination of the argon gas is the sole cause of the increased nitrogen levels in the MIM specimens. Nevertheless, it should be emphasised that despite the relatively high oxygen and nitrogen contents of the MIM specimens they show mechanical properties comparable to cast TNB-V5 as will be shown later.

Sintering conditions	Porosity [%]	Av. colony size [µm]	Mass loss [wt.%]
2 h in Ar 80 kPa	1.1	73	9.9
2 h in Ar 30 kPa	0.5	85	9.9
2 h in Ar 10 kPa	0.3	78	10.1
2 h in vacuum	0.1	74	10.5
1 h in vacuum	0.2	76	10.4

Table 2 *Porosity and average colony size of MIM-TNB-V5 sintered at 1500 °C in different atmospheres.*

3.2. Microstructure

Figure 3 shows SEM images (BSE-mode) of the cross-sections of the sintered specimens. The microstructure consists of lamellar α_2/γ colonies. EDS-analyses have shown that the light grey veils are due to residual niobium segregation. The black dots are pores and the titanium borides are visible as white needles and dots. Irrespective of the sintering condition the average colony sizes are similar and range between 73 and 85 µm (Table 2). For the two specimens sintered under vacuum for different times, it appears that there is no difference in the mean colony size. However, in contrast to our investigations a correlation between sintering time and colony size was reported in the literature for an alloy of the same B content [6]. The reason for this different behaviour could originate from the high sintering temperature of 1500 °C applied in our study. Most probably at this temperature only the β and no α phase exists (disregarding Ti borides and possibly a small amount of liquid phase). This is also obvious by comparison with Figure 4 which shows a quasi-binary section of the Ti-Al-Nb calculated by ThermoCalc using the commercial TTTiAl database for a constant content of Nb of 5 at.%. In differential scanning calorimetry (DSC) measurements a melting temperature of 1500 °C has been determined for a heating rate of 20 K/min, which agrees rather well with the calculated phase diagram.

After sintering in the β, or the β + liquid phase region, α grains nucleate during the β/α transformation when the material cools down. The size of the α grains depends mainly on the kinetics of the β/α transformation and the time that is subsequently spent in the single α phase field. Here coarsening is not hindered by the presence of β phase. In the later stages of cooling, one colony of α_2/γ lamellae is formed from each α grain. Therefore, the colony size depends on the cooling rate, especially between 1500 and 1300 °C. That is why it is necessary to pass through the α phase field in a preferably short time to avoid α grain growth during cooling. The significant influence of the cooling rate on the colony size is shown in Figure 5, which compares the microstructures of two differently cooled specimens. Both specimens were sintered for two hours under vacuum at 1500 °C. One specimen (Figure 5a) was cooled at a rate of 10 K/min while a second (Figure 5b) was cooled with an initial cooling rate of about 100 K/min within the crucial temperature range by switching off the heating of the furnace. The colony size of the slowly cooled specimen is 7 times larger than that of the more rapidly cooled specimen. In addition, the α_2/γ lamellar spacing should be influenced by the cooling rate [7] but this was not part of these investigations. However this coarsening of the microstructure led to a decrease in tensile strength from 625 to 518 MPa and in plastic elongation from 0.15 to 0.04 % (see Section 3.4).

It is known from the literature that borides which are visible as bright needles in Fig. 3 and as dark needles in the optical micrographs of Fig. 5 can serve as nucleation sites for the α phase during the β/α transformation in TiAl alloys [8] or induce equiaxed microstructures in Ti alloys [9] and thus may have a

significant influence on the microstructure of MIM TiAl alloys. However, since we did not investigate a B-free counterpart alloy, the role of borides with respect to microstructure formation in MIM-processed TiAl cannot be clarified.

The residual porosities of the sintered specimens are listed in Table 2. All specimens show a completely closed porosity. The specimens sintered under vacuum for two hours at 1500 °C (Figure 3a) show the lowest porosity with only 0.1 %. With increasing argon pressure there is a linear increase of the porosity (Figure 6) up to a level of 1.1 % for the specimen sintered under argon at 80 kPa (Figure 3d). This is probably caused by argon trapped in the pores remaining between powder particles during sintering, thereby hindering a further shrinkage of the pores [10] after closure of the pores. An increase in the sintering time apparently has only a minor effect on the residual porosity as evidenced by the fact that the porosity of the specimens sintered for 1 hour under vacuum (Figure 3b) is 0.2 %, a value which is only marginally higher than that of the specimens sintered for 2 hours under the same conditions. Due to the very low residual porosity of the parts sintered under vacuum, it cannot be totally excluded that there is a small amount of liquid phase during sintering at 1500°C which leads to this high densification.

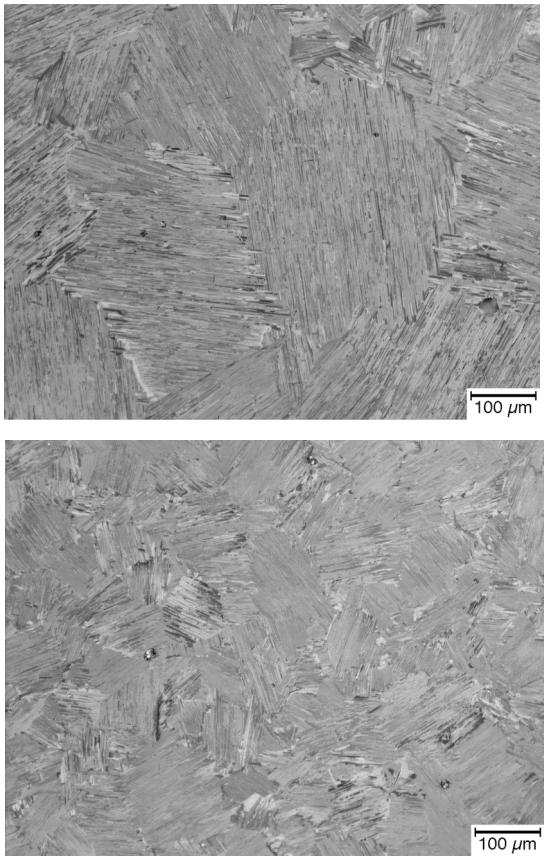

Fig. 5. *Light optical-images of cross-sections of MIM-TNB-V5 sintered 2 h at 1500 °C under vacuum and cooled down with different rates after sintering.*
(a) Cooling rate: 10 K/min. (b) Cooling rate: 100 K/min.

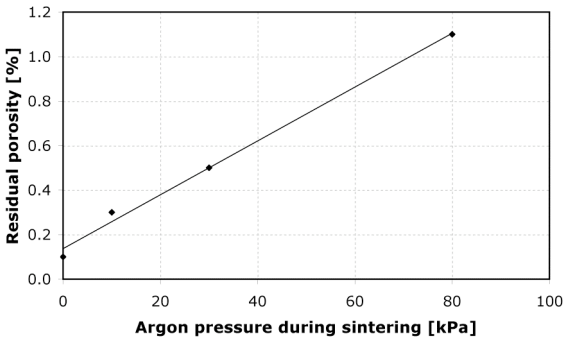

Fig. 6. *Residual porosity vs. Ar pressure during sintering of MIM-TNB-V5 (sintering time 2 h).*

3.3. Al-sublimation

Due to the high sintering temperature, the sublimation of aluminium can become a serious problem during the sintering of the TNB-V5 specimens [11] because the sintering is performed in a region of the phase diagram (Figure 4) where the present phases and the solidus temperature are very sensitive to the aluminium content. A slight temperature decrease or a small change in the aluminium content e.g. by sublimation can result in considerable changes to the phase compositions and lead to completely different sintering conditions. The temperature profile should therefore be controlled precisely.

The mass loss during debinding and sintering was measured and compared to the binder content of the green part. The mass losses of the MIM specimens are listed in Table 2. The specimens sintered two hours in argon at 30 and 80 kPa show the same mass loss of 9.9 wt. %, which is slightly less than the binder content of 10 wt. %. This difference corresponds approximately to the pick up of oxygen, nitrogen and residual carbon from the binder. With decreasing argon pressure, the mass loss increases to 10.1 wt. % for the specimens sintered for two hours in argon at 10 kPa. Specimens sintered for two hours under vacuum conditions exhibited a mass loss of 10.5 wt. %. It could be assumed that the mass loss in the latter case is mainly caused by the sublimation of aluminium. To investigate the aluminium sublimation during the sintering process, the chemical compositions of the specimens were analysed using EDS on mechanically polished cross-sections of the specimens. Line scans with a length of 500 µm were taken starting from the surface to the specimen interior.

Figure 7 shows the results of EDS line scans obtained on two MIM processed TNB-V5 specimens. Both were sintered for two hours at 1500 °C, the first one under vacuum (Figure 7a) and the second one in argon at 80 kPa (Figure 7b). Both scans seem to show a slight aluminium loss near the surface. Over the line scan taken from the specimen sintered in vacuum, a mean aluminium concentration of 43.2 at. % was determined. The deviation from the nominal Al concentration of the alloy can be attributed to the

fraction of phases present in this specimen region and to Nb segregation connected with a depletion of Al as described in section 3.2. In contrast, on the specimen sintered at 80 kPa, a mean Al concentration of 45.3 at. % was determined over the entire scan, which is very close to the nominal concentration. The slight Al loss at the surface of this specimen is surprising, because the measured mass loss corresponds to the binder content of the green part and thus does not indicate Al evaporation. Here it is noted that the analysis region must be plane for EDS measurements, i.e. directly at the surface of the cross-section specimen the EDS analyses might be not accurate due to rounding at the edges.

In order to differentiate between Al variations due to segregation and different phases and an Al loss at the surface due to evaporation, an EDS grid scan near the surface of the specimen sintered for two hours in vacuum was taken (Figure 8) from a mechanically polished sample. The scan clearly reveals a decrease in the Al concentration starting at a depth of slightly more than 100 μm below the specimen surface, i.e. far away from the specimen edge. It should be mentioned here that from vapour pressure measurements by Eckert et al. [12] an Al partial pressure of 1.35 Pa and a Ti partial pressure of 0.12 Pa can be extrapolated for the β phase of composition Ti-35 Al at a temperature of 1500 °C. Since during vacuum sintering a pressure of 10^{-3} Pa was applied, Al evaporation is plausible even if the composition of the present alloy differs significantly from the binary material investigated by Eckert et al. [12]

Furthermore, the specimens sintered for one hour under vacuum show slightly less mass loss than specimens sintered for two hours. The porosity of both specimens is completely closed and the very low porosity of the specimen sintered for only one hour under vacuum, allows the assumption that the pores close in an early stage of the sintering process. So there must be a sublimation of aluminium from the surface of the part after closure of the pores. Before closure of the pores, the aluminium surely sublimates from the bulk of the specimen, but after pore closure the aluminium sublimation is limited to the surface of the specimen. This must lead to the observed gradient of aluminium content near the surface.

This offers a possibility for process optimisation i.e. sintering in vacuum with a slight decrease in aluminium content until the pores are closed and then flushing the furnace with argon to prevent aluminium loss near the surface during the residual sintering. Because the pores are already closed, the shrinkage cannot be hindered by argon trapped in the pores.

However, since there are no obvious differences in tensile test results and microstructure – except for the porosity – between the specimens sintered in argon at different pressures and in vacuum, Al sublimation can be detected but seems to be uncritical with respect to the tensile properties, as shown in the next section.

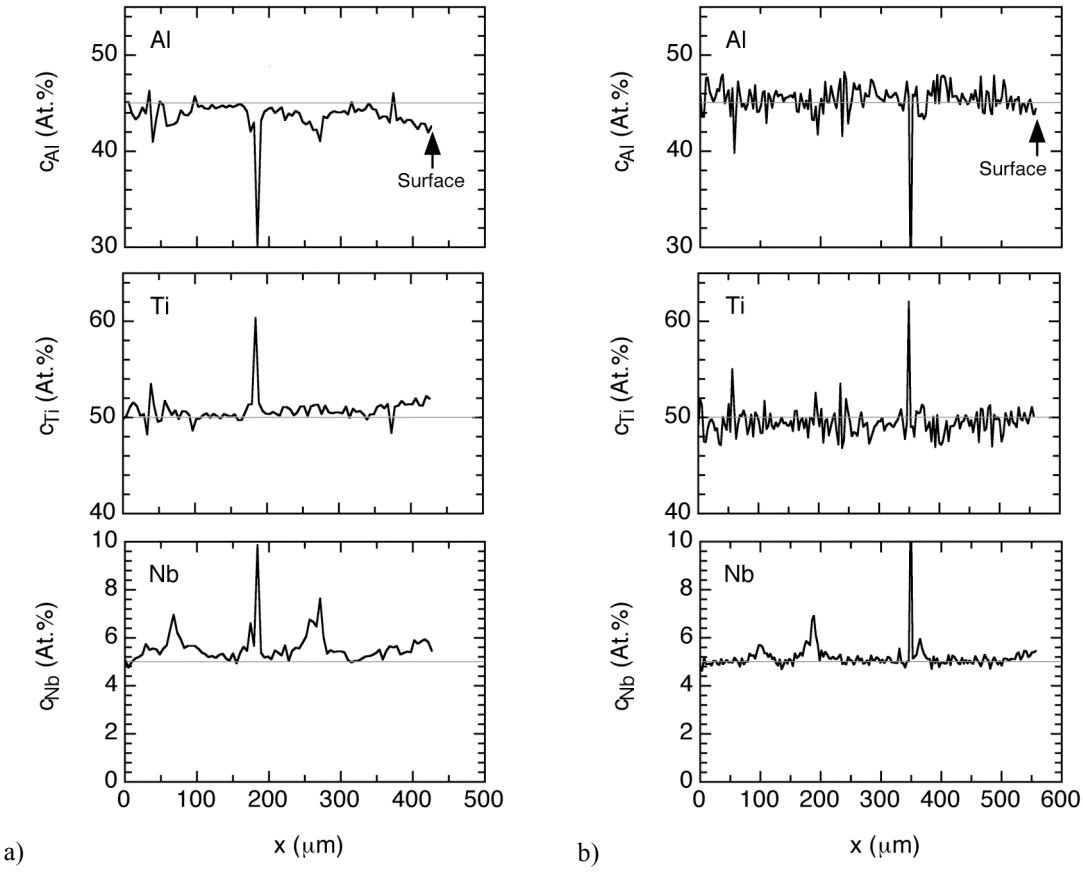

Fig. 7. *Quantitative EDS line scans of MIM-TNB-V5 parts sintered 2 h at 1500 °C. (a) Vacuum. (b) 80 kPa Ar.*

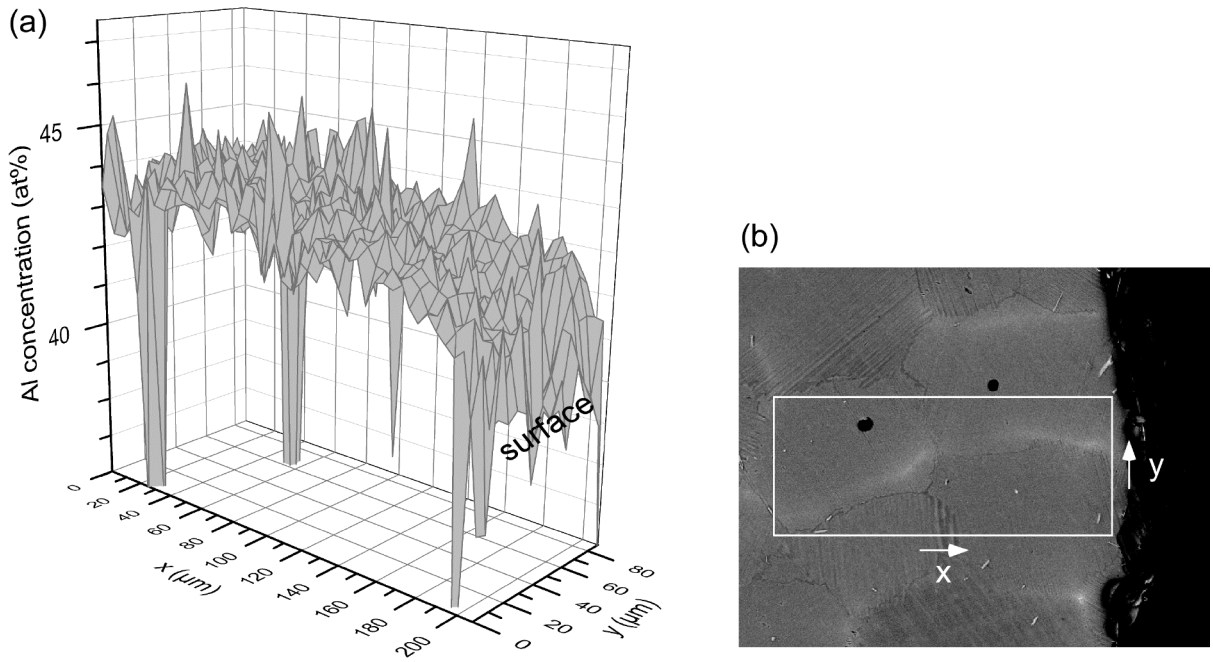

Fig. 8. *(a) Quantitative EDS grid scan over a rectangular area at the surface of a specimen sintered 2 h at 1500 °C in vacuum. (b) BSE image showing the area over which the EDS scan in (a) has been recorded.*

Sintering conditions	Cooling rate [K/min]	UTS [MPa]	ε_{pl} [%]
2 h in Ar 80 kPa	100	626 ± 11	0.19 ± 0.05
2 h in Ar 30 kPa	100	629 ± 14	0.18 ± 0.02
2 h in Ar 10 kPa	100	630 ± 17	0.17 ± 0.02
2 h in Vacuum	100	625 ± 9	0.15 ± 0.03
1 h in Vacuum	100	629 ± 20	0.19 ± 0.03
2 h in Vacuum	10	518 ± 32	0.04 ± 0.02

Table 3: *Mechanical properties of MIM-TNB-V5 sintered at 1500 °C in different atmospheres*

3.4. Tensile tests

The results of the tensile tests are listed in Table 3. For each sintering condition 6 specimens were tested. All rapidly cooled specimens – independent of the other sintering conditions – show the same mechanical properties with ultimate tensile strengths (UTS) in the range of 625 to 630 MPa and plastic elongations between 0.15 and 0.19 %. These results are certainly disappointing if the tensile properties of the TNB-V5 alloy after extrusion are considered i.e. a yield strength exceeding 1000 MPa with plastic elongation in the range 1.5 – 2.5 % [13, 14]. Similar properties were also found for rolled sheet material of the TNB-V5 alloy [15]. However, because MIM competes with near net shape processing routes, a comparison with tensile test results determined for cast specimens might be more appropriate. In the literature, no tensile properties of cast TNB-V5 material have been published to the knowledge of the authors, however at HZG an ultimate tensile strength of 705 MPa and a plastic fracture strain of 0.08 % were determined in unpublished work on cast material in the HIP condition [16]. These results are roughly comparable to other results obtained on cast material of similar alloys. Hu [17] reported a yield strength of 660 MPa and a plastic elongation of 0.3 % for the alloy Ti-44Al-8Nb-1B, whereas Hu et al. [18] found yield strengths between 602 and 638 MPa and plastic elongations in the range 0.14 – 0.4 % for various cast and heat-treated conditions of the alloy Ti-44Al-4Nb-Hf-0.1Si-0.1B. In conclusion, the excellent properties reported above for the TNB-V5 alloy have up to now only been obtained for wrought- materials.

With respect to the origin of the rather low strength and ductility there is in general a vast range of possible sources and of defects, which could play a role. MIM processing increases the complexity of the problem due to processing-related defects such as impurities, porosity, insufficient particle bonding, etc. Here it is only noted that the small differences in the impurity levels within the determined ranges (Table 1) seem to have no measurable influence on the tensile test results. As the present impurity content is significantly higher than in conventionally processed material, e.g. the cast alloys mentioned above [17, 18], the impurities certainly can affect the mechanical properties, but no conclusion is possible. The same is true for the residual porosity, which varied between 0.1 to 1.1 % and appeared to have no observable effect on the tensile properties. It is important to note that even in the specimens sintered for two hours in argon at 80 kPa which exhibited the highest porosity, the porosity is significantly lower than in other studies [6, 10], where an influence of the porosity on the mechanical properties was found. In addition, the pores have a round shape and are significantly smaller than the colony size. Thus, the ultimate tensile strength seems to be limited by other parameters which remain to be indentified. In this respect, work on microstructural refinement appears to be

interesting, e.g. by quenching after sintering or adding other alloying elements such as rare earths e.g. yttrium [19]. Aside from this question, the authors will investigate in future work the tensile properties of TNB-V5 powder compacted by HIP in order to differentiate between MIM-related defects and other parameters that affect the tensile properties.
It must be pointed out, that the specimens in this study were tested without grinding or polishing but were just shot peened with ZrO_2 before tensile testing. Nevertheless, the ultimate tensile strength of 630 MPa is the highest value reported so far for MIM-processed TiAl alloys [6, 10, 20-22].

4. Conclusions

The following conclusions can be drawn from this study:

- The TiAl alloy TNB-V5 can be processed by MIM with a residual porosity of 0.1 %, i.e. almost the theoretical density has been attained. Sintering under argon increases the porosity in proportion to the applied argon pressure but this has no effect on other microstructural parameters.
- There is a slight sublimation of aluminium when TNB-V5 is sintered under vacuum at 1500 °C. The sublimation can be successfully suppressed by sintering in an argon atmosphere of 30 kPa or more.
- UTS-values of 630 MPa and plastic elongations of 0.15 to 0.19 % were obtained at room temperature on specimens which were relatively rapidly cooled from the sintering temperature. The porosity in the range of 0.1 to 1.1 % of the sintered TNB-V5 specimens has no observable effect on the tensile strength and ductility.
- The pick up of oxygen and nitrogen does not depend on the applied argon pressure during sintering. The impurity levels after sintering range from 1140 µg/g to 1437 µg/g in oxygen and from 136 µg/g to 217 µg/g in nitrogen content. No influence of the small differences in the impurity levels within the determined ranges on the tensile properties was observed.

References

[1] M. Weimer, B. Bewlay, T. Schubert, Presentation at the 4th Intern. Workshop on Titanium Aluminides, Nuremberg, Germany, 2011.

[2] X. Wu, Intermetallics, 2006, vol. 14, 1114-1122.

[3] W. Limberg, T. Ebel, F. P. Schimansky, R. Hoppe, M. Oehring, F. Pyczak, in: Euro PM 2009, Proceedings of the International Powder Metallurgy Congress and Exhibition. Vol. 2, Copenhagen (DK), 12. - 14. 10. 2009, Shrewsbury: EPMA, 2009. p. 47-52

[4] R. Gerling, H. Clemens, F. P. Schimansky, Adv. Eng. Mat., 2004, vol. 6, p. 23.

[5] E. Aust, W.Limberg, R. Gerling, B. Oger, T. Ebel, Adv. Eng. Mat., 2006, vol. 8, p. 365-370.

[6] H. Zhang, X. He, X. Qu, L. Zhao, Mater. Sci. Eng. A 526 (2009) 31–37.

[7] M. Charpentier, A. Hazotte, D. Daloz, Mater. Sci. Eng. A 491 (2008) 321–330.

[8] U. Hecht, V. Witusiewicz, A. Drevermann, J. Zollinger, Intermetallics 16 (2008) 969-978.

[9] L.J. Huang, L. Geng, H.Y. Xu, H.X. Peng, Mater. Sci. Eng. A528 (2011) 2859-2862.

[10] R. Gerling, E. Aust, W. Limberg, M. Pfuff, F.P. Schimansky, Mater. Sci. Eng. 423 (2006) 262 - 268.

[11] T. Ebel, W. Limberg, R. Gerling, L. Stutz, R. Bormann, in: EURO PM 2007, Proceedings of the International Powder Metallurgy Congress and Exhibition. Vol. 2 Toulouse (F), 15.-17.10.2007, Shrewsbury: EPMA, 2007. 203 - 208.

[12] M. Eckert, L. Bencze, D. Kath, H. Nickel, K. Hilpert, Ber. Bunsenges. Phys.-Chem. 100 (1996) 418 – 424.

[13] F. Appel, U. Brossmann, U. Christoph, S. Eggert, P. Janschek, U. Lorenz, J. Müllauer, M. Oehring, J.D.H. Paul, Adv. Eng. Mater. 2 (2002) 699 – 720.

[14] S.L. Draper, B.A. Lerch, I.E. Locci, M. Shazly, V. Prakash, Intermetallics 13 (2005) 1014 – 1019.

[15] S.L. Draper, D. Krause, B. Lerch, I.E. Locci, B. Doehnert, R. Nigan, G. Das, P. Sickles, B. Tabernig, N. Reger, K. Rissbacher, Mater. Sci. Eng. A 464 (2007) 330 – 342.

[16] J.D.H. Paul, unpublished report, Helmholtz-Zentrum Geesthacht, Germany, 2003.

[17] D. Hu, Intermetallics 10 (2002) 851 – 858.

[18] D. Hu, H. Jiang, X. Wu, Intermetallics 17 (2009) 744 -748.

[19] L. Baohui, K. Fantao, C. Yuyong, Journal of Rare Earths 24 (2006) 352 - 356

[20] T. Shimizu, A. Kitajima, T. Sano, in: K. Kosuge, H. Nagai (Eds.), Proceedings of 2000 powder Metallurgy World Congress, Japan Society of Powder and Powder Metallurgy, Kyoto, Japan, 2000, pp. 292–295.

[21] S. Terauchi, T. Teraoka, T. Shinkuma, T. Sugimoto, Y. Ahida, in: G. Kneringer, P. Rödhammer, H. Wildner (Eds.), Proceedings of the 15th International Plansee Seminar 2000, Plansee Holding AG, Reutte, Austria, 2001, pp. 610–624.

[22] R. Gerling, F.P. Schimansky, Mater. Sci. Eng. A 329–331 (2002) 45–49.